ESRF	**Experiment title:** Hydrogen generation using TiO2-based semiconductors and Cu-Ni co-catalyst: a XAS/DRIFTS/MS analysis	**Experiment number**: **CH-4950**
Beamline: ID24	**Date of experiment**: from: 25/01/2017 to: 31/01/2017	**Date of report**: 20/07/2017
Shifts: 18	**Local contact(s)**: Debora Motta Meira	*Received at ESRF:*

Names and affiliations of applicants (* indicates experimentalists):

Mario J. Muñoz-Batista,

Marcos Fernández-García,

Instituto de Catálisis y Petroleoquímica, CSIC, C/ Marie Curie 2, 28019, Madrid (Spain).

Gerardo Colón Ibañez

Instituto de Materiales de Sevilla, CSIC, C/Américo Vespucio s/n, 41092, Sevilla (Spain)

Debora Motta Meira

ESRF, Grenoble (France).

Report:

Hydrogen production from renewables such as alcohols and water is a potentially clean means for fuel generation. Currently few methods achieve this objective. Catalytic reforming is one of them but a photocatalytic (reforming) process would be a better choice owing the significantly less demanding technological (temperature, pressure) requirements and the simplicity of the concept. Most active reforming photocatalysts contain titania as a semiconductor and noble or non-noble metals as co-catalyst.

To analyze the performance of TiO_2-based mono and bimetallic CuNi materials, at ID24/BM23 we carried out photocatalytic experiments using a Methanol:H_2O = 1:9 and measured XAS (XANES and EXAFS) as a function of the micro-beam position throughout the sample. Our experimental set-up (Figure 1) is based in a low dead volume reactor able to carry out gas-phase photocatalytic reactions under continuous flow conditions. In-situ micro-beam X-ray measurements were conducted in a fluorescence mode. In parallel, we carried out the computation of the light-matter interaction at the sample holder for our three systems (mono Cu, Ni and bimetallic Cu-Ni). The intensity decay from the sample surface is obviously wavelength dependent but the three samples showed rather similar results as a consequence of the dominant contribution of the anatase support. The wavelength averaged result for the CuNi sample as a function of the distance from the surface (depth) is presented in Figure 1. From this result it becomes obvious that a beam spot well below 5 microns is required to obtain meaningful results (99.9 % of light is absorbed within the first 2.5 microns). We thus carried out the experiment using a 3 x 3 microms focal spot.

Photo-catalytic activity measurements indicate that the bimetallic CuNi powder presents a strong synergistic interaction with respect to the monometallic counterparts (enhancement ratios x2 and x10 in hydrogen production with respect to Cu and Ni samples). The non-noble co-catalyst(s) physico-chemical properties as a function of the sample depth from the surface of the materials (where light incides in the solid) were analyzed with the help of XAS techniques. First, *Operando* XANES spectra at the Cu and Ni K-edges under illumination and dark conditions were evaluated in independent experiments

Examining Cu K-edge XANES results at the “surface” position (defining in this case the surface as the sample region light effect has chemical consequences; under 3 microns) we observed differences for samples pre-treated with the gas atmosphere. Among the positions scanned in the study is the only one that suffers differences when illuminated, irrespective of the (copper-containing) sample measured. Concretely,

both the monometallic Cu and bimetallic CuNi suffer an oxidation process from an initially (previously to the light switching on) fully reduced state. Just below the surface, the state of copper is reduced up to a depth where the effect of the gas phase (more concretely of the reductant alcohol) on the solids disappears. Contrarily to the copper case, XANES demonstrates that Ni maintains always a dominant Ni(II) oxidized state at the surface and bulk positions of the catalysts, with negligible changes within dark or illuminated conditions.

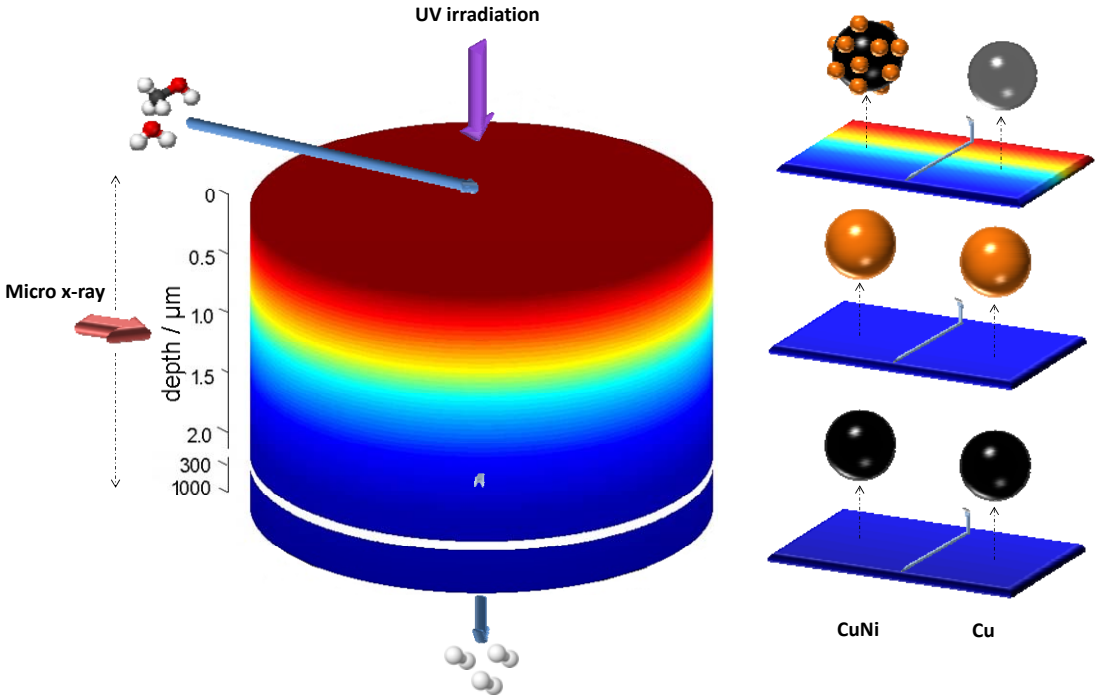

Fig.1. Schematic view of the sample and experimental conditions. The sample is confined in a cell which allows simultaneous gas phase treatment and illumination from to top side. Arrows show the direction of the gas flow, illumination and incident X-ray micro-beam. The X-ray micro-beam probes non noble metal chemical states and structure as a function of the depth from the surface. Panels at the right hand depict the most relevant metal-containing phases (Cu(0) brown color; Cu(II) black color) for different depths described by the light intensity received. Cu and CuNi samples are considered.

Factor Analysis was utilized to shed more light into the oxidation process tacking place under illumination for the copper component. Figure 2 summarizes the results of the study which confirms the presence of a Cu(II) oxidation state only in the illuminated zone of the materials. More concretely, ca. 38 and 11 mol. % of copper appears in a oxidic Cu(II) environment for, respectively, Cu and CuNi samples, while the rest of copper remains as Cu(0). So, a first difference between our copper-containing samples concerns the degree of oxidation. The XANES spectra corresponding to the pure chemical species (Cu(0) band Cu(II)) expands the differences between the samples. As can be seen in Figure 3 subtle differences are presented in the Cu(II) state but more acute ones are visible in the Cu(0) state. The typical shape of the Cu foil is reasonable followed by the Cu sample. The CuNi displays a typical 1s→ 4p pre-edge transition but the characteristic valley between the 5sp resonances is less marked as a consequence of the (energy) smearing of the corresponding continuum states, a typical effect of alloying. Such alloys is almost not detected at the Ni K-edge indicating the limited Ni content of such phase (well below 10 at. % of total Ni).
The analysis of the supported phases was completed with the structural view rendered by *operando* EXAFS. Absence of significant differences at the Ni K-edge is observed between Ni and CuNi samples under dark or illumination conditions. Ni is not responding to the gas phase or illumination to a significant degree. At the Cu K-edge, comparative analysis of the EXAFS fitting results for the Cu and CuNi samples can be carried at the surface and below it (Figure 3). At the surface (see bottom panels of Figure 3) the Cu sample displays a metallic-type Cu-Cu contribution (distance characteristic of the metal) absent in the CuNi sample. This is qualitatively observed in the imaginary part of the Fourier Transform. Combined with the XANES results indicating the presence of Cu(0) in both catalysts, the joint analysis proofs a different contact between the

Cu(0) and the Cu(II) phases detected within the surface region of the catalysts. As Cu is fully reduced before light switching on, illumination renders a core-shell type structure (depicted in Figure 1) for the Cu sample. For the CuNi sample, zerovalent Cu atoms do not show Cu-Cu interactions, indicating that they are essentially atomically dispersed in a Cu(II) matrix. This is likely an effect of Ni (limited) presence in the initial zerovalent phase as no size effect is expected (Figure 3). The chemical and structural differences between the two (Cu and CuNi) samples at the surface are graphically summarized in Figure 1. Below the surface, some size differences between the Cu and CuNi samples can be encountered. Although detectable, they do not significantly change the dispersion of the corresponding non-noble metal phase as a consequence of the small metal particle size in both samples, always below 1.5 nm.

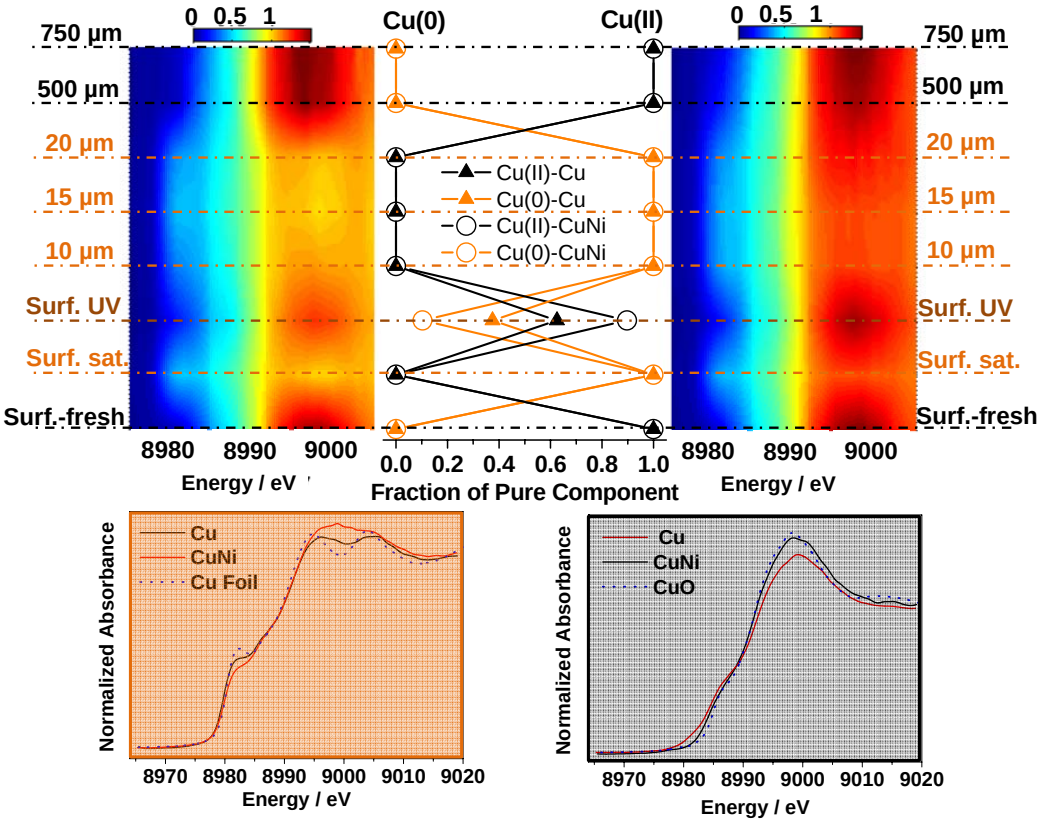

Fig.2. Contour plot of Cu K-edge XANES spectra obtained under illumination for the Cu (left) and CuNi(right) samples. For the surface position, the two previous states (fresh sample and after gas contact) are included. Concentration profiles (central part) and XANES spectra (lower panels) corresponding to pure chemical species obtained from Principal Component Analysis are included. Colors in the central panel are assigned to pure species: black, Cu(II); orange, Cu(0).

The study thus shows that copper vividly responds under *operando* conditions while nickel has a significantly lower response and thus chemical role in bimetallic systems. The higher activity of copper is a known fact in the literature and is here corroborated by the catalytic experiments. Focusing on the comparison of copper containing catalysts, the results are however radically different from previous studies based on a conventional use of XPS, TPD or EXAFS. All these previous reports indicate the significance of copper reduced states in photo-activity. This agrees with our results as an average of the sample subjected to the gas phase contact (see Figure 1), but it is not certainly the view coming from the sample part upon the simultaneous influence of light and gas phase, a fact achievable in this study through the use of a X-ray micro-beam and the understanding of the light-matter interaction at the measurement cell. For the Cu sample we observed a core-shell structure where the metallic copper facilitates the electron handling properties while the surface chemical role is played by the oxidized copper phase. Larger photo-activity is nevertheless obtained for the CuNi sample, with a secondary chemical role played by nickel. In this case, the copper-rich component is composed by metallic entities with limited atomicity (according to EXAFS) finely dispersed into a copper oxide matrix (according to XANES). As a result, the key effect of nickel is to shape the phase

contact among copper phases and to control the electronic and structural properties of both (but particularly the metallic type state), leading to a synergistic interaction with significant influence in photo-activity. Thus, the combination of truly *operando* micro-XANES and –EXAFS at relevant light/X-ray beam probe "lengths" unveils a new perspective in both monometallic and bimetallic catalysts, which can be useful in a significant number of photocatalytic studies.

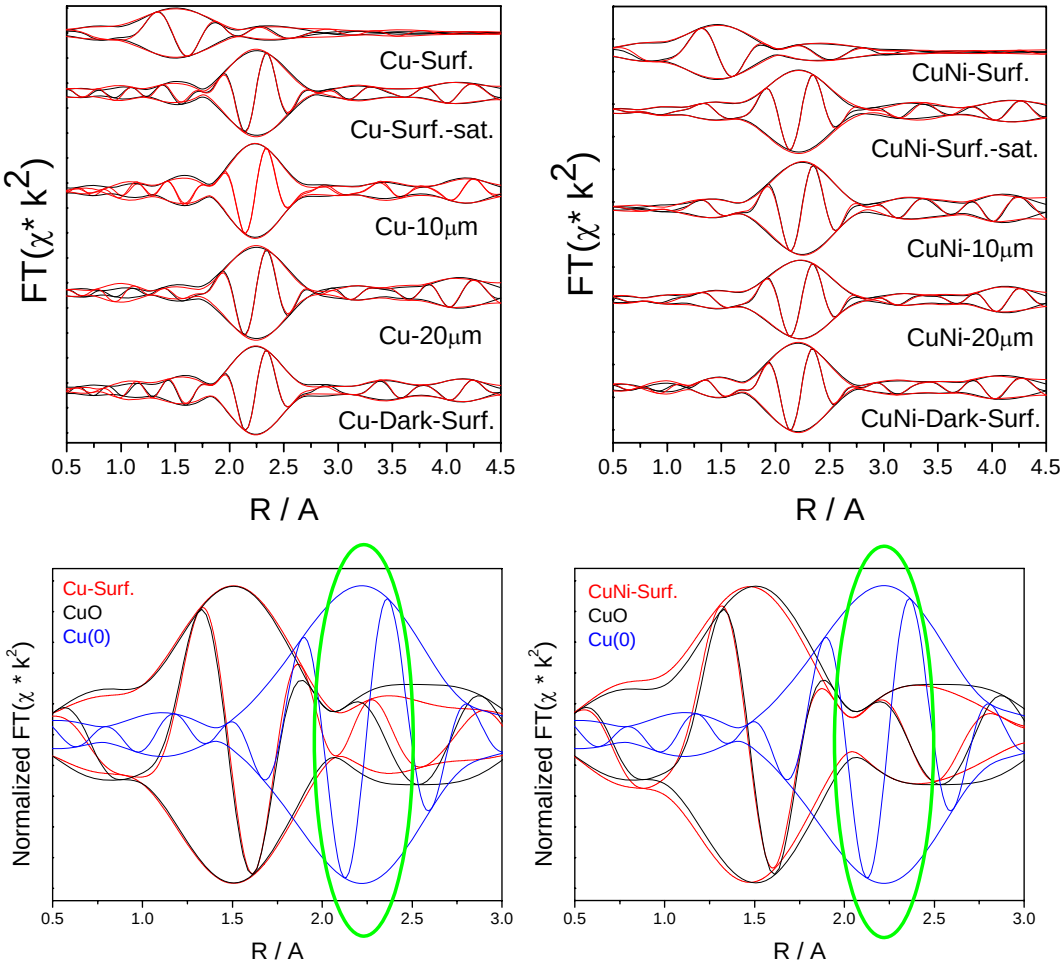

Fig.3. Upper panels: Fourier Transform magnitude and imaginary part of the Cu K-edge EXAFS signals (red curves) obtained for the Cu and CuNi samples. Fitting results (black curves) are also included. Lower panels; low-R detail of the Fourier Transform obtained at the surface of the materials (red curve). The lower panel figures include the normalized Cu foil (blue curve) and CuO (black curve) references.

Finally, we would like to acknowledge Drs D. Meira Motta and O.Mathon for supporting the experiments carried out at ID24/BM23.